Twin image removal in X-ray fluorescence holography with two energies

CHEN Miao-Xin(陈淼鑫)[1)]   LI Zheng(李政)[2)]

(Key Laboratory of Particle & Radiation Imaging (Tsinghua University), Ministry of Education,
Department of Engineering Physics, Tsinghua University, Beijing 100084, China)

Abstract   In the last decade, X-ray fluorescence holography has been developed for the study of 3D atomic arrangements in solids. However, it encounters the twin image problem which may disturb the reconstructed atomic images. In this paper, the formation of twin image is discussed and we propose a modified two-energy algorithm to remove the twin image. The simulation shows that the method is valid and more efficient than the multiple-energy algorithm proposed by Barton.

Key words   X-ray, holography, twin image

PACS   78.70.En, 42.40.-i

1   Introduction

X-ray fluorescence holography (XFH) is a developing technique which can directly provide a three dimensional imaging of local atomic structures, which is fundamental in physics, chemistry and material science. XFH is based on holography imaging technique invented by Gabor in 1948[1]. The resolution of holography is determined by the numerical aperture (NA). Source with small size will produce a diffraction cone beam with big enough NA and the diffraction beam could form the hologram with the same NA after the interference with the scattering beam. Only such a big NA could obtain atomic-scale resolution, so the conventional holography cannot reach the resolution of atomic-scale because of the limitation of the size of source. In 1986, Szöke[2] first suggested that a photo-excited atom emitting fluorescent X-ray was an ideal coherent source to form hologram and proposed the concept of XFH which is in fact a kind of conventional Fourier holography with atomic-scale resolution. There are two types of XFH: the "normal XFH" and the "inverse XFH" which corresponds to the inverse Fourier holography. In the normal mode as shown in Fig. 1(a), the fluorescence from emitter atoms directly arriving at the detector constitutes the holographic reference wave, and the fluorescence scattered by neighboring atoms acts as the object wave.

A hologram pattern can be obtained by moving the detector around the sample. The first experimental realization of XFH was performed by Tegze and Faigel in 1996[3]. Fig. 1(b) illustrates the inverse mode[4]
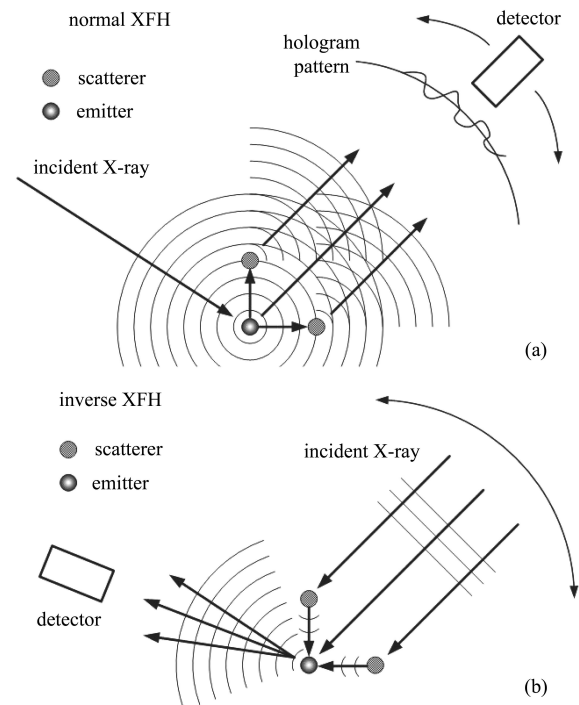

Fig. 1.   Illustration of normal XFH (a) and inverse XFH (b).

which is the optical reciprocity of the normal, the monochromatic incident X-ray is the reference wave and the scattered X-ray is the object wave. In inverse XFH the hologram can be recorded at any incident energy above the absorption edge of the emitter atom so multiple energy X-ray holography (MEXH) can be carried out.

The atomic structure can be reconstructed from the hologram pattern with the widely used algorithm proposed by Barton[5]. However, the holographic reconstruction at a single energy will suffer from the twin image. It is difficult to distinguish the real image and its twin image at the centro-symmetric position. Even cancellation may happen if the sample has centro-symmetric structure because the real and twin image occupy the same position and the interference of them result in the image intensity's oscillation depending on the atom position and the wavelength[6]. In order to solve the problem, Barton also proposed the popular multiple energy algorithm[7] in which holograms recorded at different energies are combined to suppress the twin images. It is recommended that 10—15 energies are required to obtain an acceptable reconstruction[6].

In this paper the formation of twin image is discussed and we propose a modified two-energy algorithm that only two energies are needed. A special model is used to test our algorithm and the simulation result shows that the algorithm is feasible and more efficient compared with Barton's method.

2 Twin image problem

2.1 Formation of twin image

According to Ref. [8], the hologram is given by:

$$\chi(\boldsymbol{k}) = \sum_j \chi_j(\boldsymbol{k}) =$$

$$2\mathrm{Re}\sum_j \frac{f_j(\theta_{\boldsymbol{r}_j,\boldsymbol{k}})}{r_j}\exp\left[i(r_j k - \boldsymbol{r}_j\cdot\boldsymbol{k})\right], \quad (1)$$

where $\boldsymbol{k}$ is the wave vector and $\boldsymbol{r}_j$ is the position vector of the scatterer with respect to the emitter, and $f_j(\theta_{\boldsymbol{r}_j,\boldsymbol{k}})$ is the atomic scattering factor depending on the angle between $\boldsymbol{r}_j$ and $\boldsymbol{k}$. The atomic scattering factor includes the polarization factor which will influence the atomic images reconstructed[9]. But in the case of normal XFH, the fluorescence emitted by atoms is unpolarized, so the polarization factor can be simplified to $P_0(\theta) = (1+\cos^2\theta)/2$ as in Ref. [10]. In our present study this situation is concerned and the case of polarization will be taken into account in further work.

The hologram $\chi(\boldsymbol{k})$ can be reconstructed with

Barton's single-energy algorithm via[5]:

$$U(\boldsymbol{r}) = \iint \chi(\boldsymbol{k})\exp(-i\boldsymbol{k}\cdot\boldsymbol{r})\mathrm{d}\sigma_k. \quad (2)$$

First, let us consider the situation that a single scattering atom locates at $\boldsymbol{r} = +\boldsymbol{a}$ (Fig. 2(a)), the reconstructed image can be written as:

$$U(\boldsymbol{r}) \propto \exp(-ika)\iint f^*(\theta_+)\exp\left[-i\boldsymbol{k}\cdot(\boldsymbol{r}-\boldsymbol{a})\right]\mathrm{d}\sigma_k +$$

$$\exp(ika)\iint f(\theta_+)\exp\left[-i\boldsymbol{k}\cdot(\boldsymbol{r}+\boldsymbol{a})\right]\mathrm{d}\sigma_k, \quad (3)$$

where θ_+ is the scattering angle between $+\boldsymbol{a}$ and $\boldsymbol{k}$. The first term corresponds to the real image and the second term is the twin image. $U(\boldsymbol{r})$ peaks at $\boldsymbol{r} = +\boldsymbol{a}$ and $\boldsymbol{r} = -\boldsymbol{a}$ so the twin image appears at $\boldsymbol{r} = -\boldsymbol{a}$ (Fig. 2(a)).
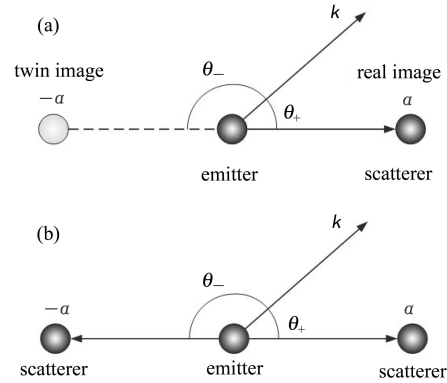

Fig. 2. Single-scatterer model (a) and two-scatterer model (b).

2.2 Image cancellation

For a pair of scattering atoms located at $\boldsymbol{r} = \pm\boldsymbol{a}$ (Fig. 2(b)), the reconstructed atomic image at the special point $\boldsymbol{r} = +\boldsymbol{a}$ would be the superposition of the real image of the atom at $+\boldsymbol{a}$ and the twin image of the atom at $-\boldsymbol{a}$:

$$U(\boldsymbol{r}=\boldsymbol{a}) \propto \exp(-ika)\iint f^*(\theta_+)\mathrm{d}\sigma_k +$$

$$\exp(ika)\iint f(\theta_-)\mathrm{d}\sigma_k, \quad (4)$$

where $\theta_- = \pi - \theta_+$. For the geometry it is satisfied that

$$\iint f(\theta_+)\mathrm{d}\sigma_k = \iint f(\theta_-)\mathrm{d}\sigma_k. \quad (5)$$

In this case, the atomic image at $\boldsymbol{r} = +\boldsymbol{a}$ can be written as:

$$U(\boldsymbol{r}=\boldsymbol{a}) \propto \cos(ka)\iint \mathrm{Re}\left[f(\theta_+)\right]\mathrm{d}\sigma_k -$$

$$\sin(ka)\iint \mathrm{Im}\left[f(\theta_+)\right]\mathrm{d}\sigma_k. \quad (6)$$

Thus the image cancellation happens when

$$\tan(ka) = \frac{\iint \mathrm{Re}\,[f(\theta_+)]\,\mathrm{d}\sigma_k}{\iint \mathrm{Im}\,[f(\theta_+)]\,\mathrm{d}\sigma_k}. \tag{7}$$

In the case of X-ray scattering, the imaginary part of f is very small and the cancellation condition in Eq. (7) can be simplified to $ka = (2n+1)\pi/2$, where n is a non-zero integer. So when $|a| = (2n+1)\lambda/4$, pairs of atoms at $\boldsymbol{r} = \pm\boldsymbol{a}$ cannot be seen in the reconstructed image. On the other hand, $U(\boldsymbol{r} = \boldsymbol{a})$ will be enhanced when $ka = n\pi$ (see Eq. (6)). The real image combined with the twin image makes the image intensity oscillate with the change of atomic distance and wavelength.

2.3 Multiple-energy algorithm

It is clear that if the twin image is eliminated, the problem above will be circumvented. From Eq. (3), we can see that the appearance of the twin image is due to the balance of the real image and its twin one. So if the balance is broken, only the real image can be expected. This is how Barton's multiple-energy algorithm works.

Inserting Eq. (3) into Barton's algorithm[7, 8]

$$U(\boldsymbol{r}) = \int k^2 \iint \chi(\boldsymbol{k}) \exp\left[-\mathrm{i}(\boldsymbol{k}\cdot\boldsymbol{r} - kr)\right] \mathrm{d}\sigma_k \mathrm{d}k, \tag{8}$$

it gives:

$$\begin{aligned}U(\boldsymbol{r}) \propto &\int k^2 \exp\left[\mathrm{i}k(r-a)\right] \times \\ &\iint f^*(\theta_+)\exp\left[-\mathrm{i}\boldsymbol{k}\cdot(\boldsymbol{r}-\boldsymbol{a})\right]\mathrm{d}\sigma_k \mathrm{d}k + \\ &\int k^2 \exp\left[\mathrm{i}k(r+a)\right] \times \\ &\iint f(\theta_+)\exp\left[-\mathrm{i}\boldsymbol{k}\cdot(\boldsymbol{r}+\boldsymbol{a})\right]\mathrm{d}\sigma_k \mathrm{d}k. \end{aligned} \tag{9}$$

Apparently the twin image at $\boldsymbol{r} = -\boldsymbol{a}$ is suppressed as a result of the sum of random phase while the real image at $\boldsymbol{r} = +\boldsymbol{a}$ retains.

3 Two-energy algorithm

Although Barton's method is valid and widely used nowadays, we note that the reconstruction improves with the increasing of the number of holograms used, and 10—15 holograms are recommended[6]. This consumes more time of measurement and reconstruction. Here we introduce a modified algorithm that needs only two energies. The two-energy algorithm was once proposed by Nishino[11] in 2002, the method we present here is a modified form of that, we

fully use the information of the holograms recorded at two different energies.

Similarly we take the consideration that only a scattering atom locates at $\boldsymbol{r} = +\boldsymbol{a}$ (Fig. 2(a)). From Eq. (3) we arrive at:

$$\begin{aligned}U(\boldsymbol{r} = \boldsymbol{a}) &\propto \exp(-\mathrm{i}ka)\iint f^*(\theta_+)\mathrm{d}\sigma_k = \\ &G^*(k)\exp(-\mathrm{i}ka), \end{aligned} \tag{10}$$

$$U(\boldsymbol{r} = -\boldsymbol{a}) \propto \exp(\mathrm{i}ka)\iint f(\theta_+)\mathrm{d}\sigma_k = G(k)\exp(\mathrm{i}ka), \tag{11}$$

where $G(k)$ is defined as:

$$G(k) = \iint f(\theta_+)\mathrm{d}\sigma_k. \tag{12}$$

Taking account of two different wave-numbers, k_1 and k_2, we give the function

$$\begin{aligned}V_{k_1,k_2}(\boldsymbol{r}) = \;&2U_{k_1}(\boldsymbol{r})U_{k_2}(\boldsymbol{r}) - U_{k_1}^2(\boldsymbol{r})\exp\left[\mathrm{i}(k_2 - k_1)r\right] - \\ &U_{k_2}^2(\boldsymbol{r})\exp\left[\mathrm{i}(k_1 - k_2)r\right]. \end{aligned} \tag{13}$$

If the difference of the atomic scattering factor f at k_1 and k_2 is small enough, then $2\bar{G} = G(k_1) + G(k_2) \gg G(k_1) - G(k_2)$ and $G(k_1) \approx G(k_2)$ is approximately satisfied[11], so

$$\begin{aligned}V_{k_1,k_2}(\boldsymbol{r} = \boldsymbol{a}) \propto \;&2G^*(k_1)G^*(k_2)\exp\left[-\mathrm{i}(k_1 + k_2)a\right] - \\ &G^*(k_1)G^*(k_1)\exp\left[\mathrm{i}(k_2 - 3k_1)a\right] - \\ &G^*(k_2)G^*(k_2)\exp\left[\mathrm{i}(k_1 - 3k_2)a\right] \approx \\ &\bar{G}^{*2}\exp\left[-\mathrm{i}(k_1 + k_2)a\right] \times \\ &\left[2 - \exp(2\mathrm{i}\delta ka) - \exp(-2\mathrm{i}\delta ka)\right] = \\ &4\bar{G}^{*2}\exp\left[-\mathrm{i}(k_1 + k_2)a\right]\sin^2(\delta ka), \end{aligned} \tag{14}$$

$$\begin{aligned}V_{k_1,k_2}(\boldsymbol{r} = -\boldsymbol{a}) \propto \;&2G(k_1)G(k_2)\exp\left[\mathrm{i}(k_1 + k_2)a\right] - \\ &G(k_1)G(k_1)\exp\left[\mathrm{i}(k_1 + k_2)a\right] - \\ &G(k_2)G(k_2)\exp\left[\mathrm{i}(k_1 + k_2)a\right] \approx 0, \end{aligned} \tag{15}$$

where $\delta k = k_2 - k_1$.

The new image function shows that the twin image at $\boldsymbol{r} = -\boldsymbol{a}$ is almost eliminated while the real image $|V_{k_1,k_2}(\boldsymbol{r} = \boldsymbol{a})|$ remains as long as $|\sin(\delta ka)|$ is big enough. In practice, one can choose two energies with the difference of several hundred eV, for example, 400 eV. In this case, in the range of r ($1.2\,\text{Å} \leqslant r \leqslant 14.3\,\text{Å}$, $|\sin(\delta ka)| \geqslant 1/4$) only the real images are retrieved. The method presented here is almost the square of Nishino's method after approximation but different from that, because we use quadratic polynomial to suppress the twin image thoroughly.

4   Simulation and discussion

In order to test our method, a special model including 8 Fe atoms is used (Fig. 3(a)), the lattice constant a=2.8662 Å. The atom in the center of the cube is the emitter and the others are the scattering atoms. Fig. 3(b) shows the expected reconstructed image with Barton's single-energy algorithm, the emitter is removed because of the method itself and the twin images are marked.
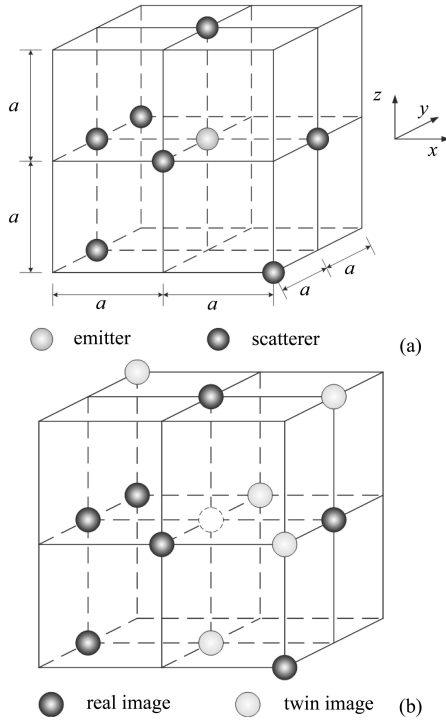

Fig. 3.   8-atom Fe cluster model (a) and the expected reconstructed image with single-energy algorithm (b).

In the following simulation, a Fast Fourier Transform (FFT) algorithm based on Ref. [12] is used to speed up the reconstruction. We first reconstruct the z=0 plane at k=18.1 Å^{-1} and k=18.6 Å^{-1} respectively. According to the previous discussion, the cancellation condition is satisfied when k=18.1 Å^{-1} for atoms $(a,0,0)$ and $(-a,0,0)$ while they are enhanced when k=18.6 Å^{-1}. And the twin images at $(a,-a,0)$ and $(0,a,0)$ appear due to the problem of single-energy algorithm. As shown in Fig. 4, the reconstruction agrees with the expectation.
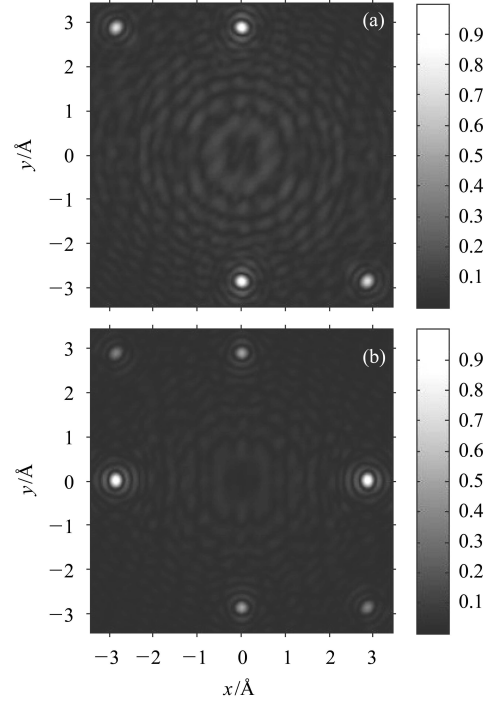

Fig. 4.   Reconstructed image at z=0, (a) k=18.1 Å^{-1}, (b) k=18.6 Å^{-1} (The gray scale bar indicates the normalized magnitude of the reconstructed image).

Figures 5, 6 and 7 give the reconstructed atomic images at $z=a$, z=0 and $z=-a$ respectively. The reconstruction utilizing single-energy, multiple-energy and our two-energy algorithm are shown for comparison. Referring to Fig. 3(b), it is clear that the twin image problems cannot be avoided if we simply apply Barton's single-energy algorithm while the multiple-
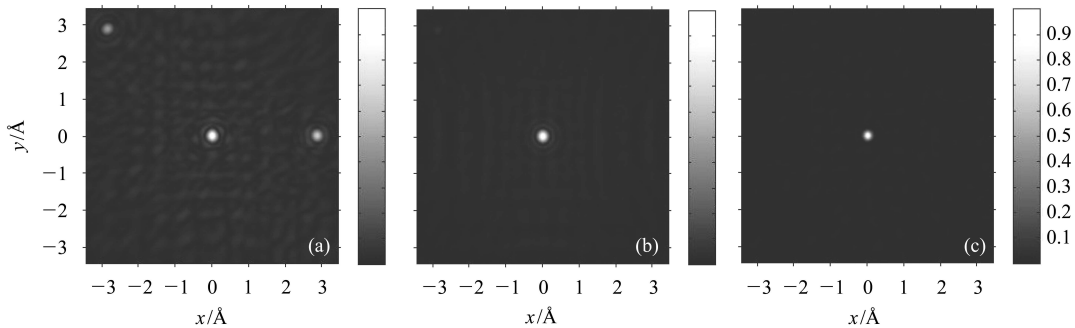

Fig. 5.   Images reconstructed at $z=a$ plane, (a) Single-energy reconstruction at k=19.1 Å^{-1}; (b) Multiple-energy reconstruction from k=16.1 Å^{-1} to k=21.1 Å^{-1} with dk=0.5 Å^{-1}; (c) Two-energy reconstruction with k_1=18.1 Å^{-1} and k_2=18.3 Å^{-1}.
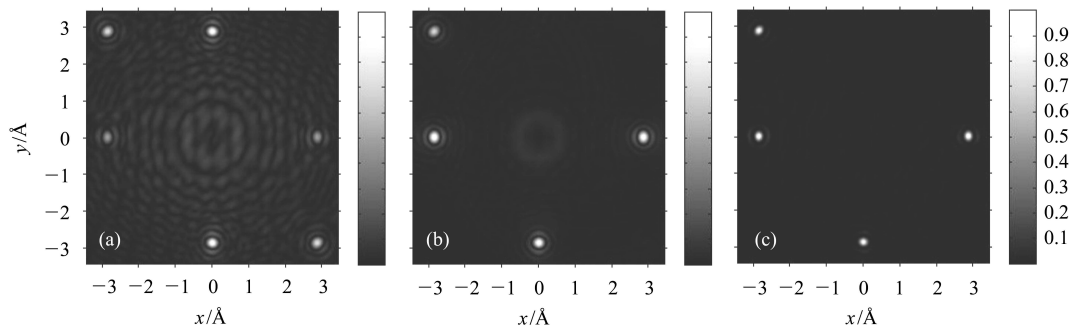
Fig. 6.   As in Fig. 5, but for images at $z=0$ plane.
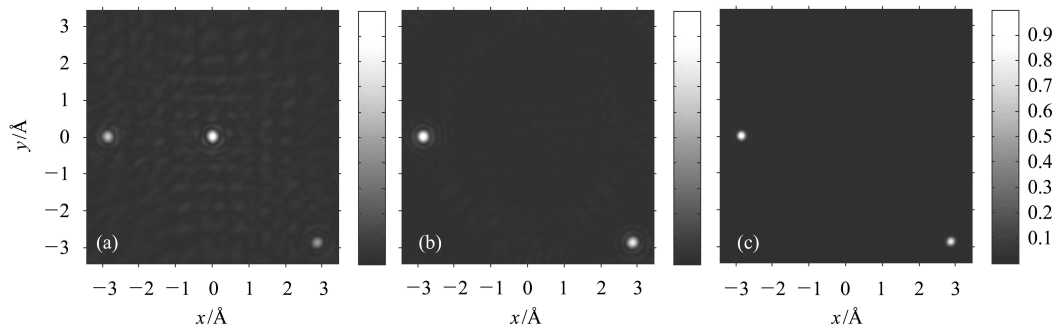

Fig. 7.   As in Fig. 5, but for images at $z = -a$ plane.

energy and two-energy methods can obtain twin image free reconstruction. Comparing Fig. 6(c) with Fig. 4(a), we can see that the disappeared atoms (Fig. 4(a)) emerge in their positions (Fig. 6(c)) as a result of the elimination of the twin images, the twin images of atom $(-a,a,0)$ and $(0,-a,0)$ are removed as well. Furthermore, we find that the atom at $(-a,a,0)$ (Fig. 6) and the atom at $(a,-a,-a)$ (Fig. 7) reconstructed with two-energy algorithm are more bright and clear than that with multiple-energy algorithm. This is because the number of wave-number used in Eq. (8) is finite.

The simulation shows that the two-energy method successfully removes the problematic twin images and the true atoms are visible clearly. As the multiple-energy algorithm requires more holograms recorded at different energies, it is evident that the two-energy algorithm is more efficient. In practice this is useful and experiments become easier by detecting only two different fluorescence intensities, for example, K_α and K_β, in normal XFH[11].

5   Conclusion

X-ray fluorescence holography is a promoting technique for structure determination. In this paper, the twin image problem in XFH is discussed and a modified two-energy twin image removal algorithm is proposed. The theoretical simulation shows that our method is valid and more efficient than Barton's. Furthermore, by applying two-energy algorithm, it is possible that most experiments finished at synchrotron radiation facilities nowadays may be performed using laboratory X-ray generators[13] because the tunable-energy wave source becomes unnecessary and the characteristic X-rays from generators will accomplish the measurement. This will lead to the real application in the near future.

References

1 Gabor D. Nature, 1948, **161**: 777—778
2 Szöke A. Short Wavelength Coherent Radiation: Generation and applications. Attwood D T, Boker J eds. New York: AIP, 1986. 361—367
3 Tegze M, Faigel G. Nature, 1996, **380**: 49—51
4 Gog T, Len P M, Materlik G et al. Phys. Rev. Lett., 1996, **76**(17): 3132—3135
5 Barton J J. Phys. Rev. Lett., 1988, **61**(12): 1356—1359
6 Len P M, Thevuthasan S, Fadley C S et al. Phys. Rev. B, 1994, **50**(15): 11275—11278

7 Barton J J. Phys. Rev. Lett., 1991, **67**(22): 3106—3109
8 Faigel G, Tegze M. Rep. Prog. Phys., 1999, **62**: 355—393
9 Len P M, Gog T, Novikov D et al. Phys. Rev. B, 1997, **56**(3): 1529—1539
10 Tegze M, Faigel G. J. Phys.: Condens. Matter, 2001, **13**: 10613—10623
11 Nishino Y, Ishikawa T, Hayashi K et al. Phys. Rev. B, 2002, **66**: 092105
12 WANG J Y, ZHU P P, ZHENG X et al. Acta Phys. Sin., 2005, **54**(3): 1172—1177 (in Chinese)
13 Takahashi Y, Hayashi K, Nishiki N et al. J. Mater. Res., 2003, **18**(6): 1471—1473